

This article was downloaded by: [122.118.5.156]

On: 10 October 2014, At: 19:32

Publisher: Taylor & Francis

Informa Ltd Registered in England and Wales Registered Number: 1072954 Registered office: Mortimer House, 37-41 Mortimer Street, London W1T 3JH, UK



Structure and Infrastructure Engineering: Maintenance, Management, Life-Cycle Design and Performance

Publication details, including instructions for authors and subscription information:
<http://www.tandfonline.com/loi/nsie20>

Behaviour of segmental pipeline protective vaults subjected to fault offset

Chi-Chin Tsai^a, Philip Meymand^b, Ethan Dawson^b & Stephanie A. Wong^c

^a Department of Civil Engineering, National Chung Hsing University, 250 Kuokuang Road, Taichung, Taiwan

^b URS Corporation, 1333 Broadway, Suite 800, Oakland, CA 94612, USA

^c San Francisco Public Utilities Commission, 525 Golden Gate Avenue, 11th Floor, San Francisco, CA 94102, USA

Published online: 08 Oct 2014.

To cite this article: Chi-Chin Tsai, Philip Meymand, Ethan Dawson & Stephanie A. Wong (2014): Behaviour of segmental pipeline protective vaults subjected to fault offset, Structure and Infrastructure Engineering: Maintenance, Management, Life-Cycle Design and Performance, DOI: [10.1080/15732479.2014.964733](https://doi.org/10.1080/15732479.2014.964733)

To link to this article: <http://dx.doi.org/10.1080/15732479.2014.964733>

PLEASE SCROLL DOWN FOR ARTICLE

Taylor & Francis makes every effort to ensure the accuracy of all the information (the "Content") contained in the publications on our platform. However, Taylor & Francis, our agents, and our licensors make no representations or warranties whatsoever as to the accuracy, completeness, or suitability for any purpose of the Content. Any opinions and views expressed in this publication are the opinions and views of the authors, and are not the views of or endorsed by Taylor & Francis. The accuracy of the Content should not be relied upon and should be independently verified with primary sources of information. Taylor and Francis shall not be liable for any losses, actions, claims, proceedings, demands, costs, expenses, damages, and other liabilities whatsoever or howsoever caused arising directly or indirectly in connection with, in relation to or arising out of the use of the Content.

This article may be used for research, teaching, and private study purposes. Any substantial or systematic reproduction, redistribution, reselling, loan, sub-licensing, systematic supply, or distribution in any form to anyone is expressly forbidden. Terms & Conditions of access and use can be found at <http://www.tandfonline.com/page/terms-and-conditions>

Behaviour of segmental pipeline protective vaults subjected to fault offset

Chi-Chin Tsai^{a*}, Philip Meymand^{b1}, Ethan Dawson^{b2} and Stephanie A. Wong^{c3}

^aDepartment of Civil Engineering, National Chung Hsing University, 250 Kuokuang Road, Taichung, Taiwan; ^bURS Corporation, 1333 Broadway, Suite 800, Oakland, CA 94612, USA; ^cSan Francisco Public Utilities Commission, 525 Golden Gate Avenue, 11th Floor, San Francisco, CA 94102, USA

(Received 15 February 2014; final version received 28 June 2014; accepted 20 July 2014)

The San Francisco Public Utilities Commission is currently undertaking a seismic upgrade of Bay Division Pipelines (BDPLs) Nos. 3 and 4 located in Fremont, California. To improve the reliability of the pipelines at a crossing of the Hayward Fault, a new pipeline (BDPL No. 3X) will be constructed in a segmental reinforced concrete vault with flexible connection joints that can accommodate lateral offsets and compressive deformations during a significant fault rupture. FLAC 3D finite difference analysis was performed to enhance the understanding of the soil–structure interaction behaviour of this special design. The analysis focused on the behaviour of the segmental concrete vault when subjected to up to 2.0 m (6.5 ft) lateral fault movement. The effects of fault intersection angle, fault location, soil strength, backfill type and connection joint size on the performance of the segmental concrete vault were also evaluated. Numerical results show that the movement of the vault developed gradually without sudden or concentrated deformation in response to the increasing fault displacement. Hence, the articulated vault design can withstand significant lateral offset and compressive deformation during fault rupture through the relative slip and rotation of the flexible connection joints.

Keywords: segmental vaults; pipelines; seismic design; numerical simulation; soil–structure interaction; fault offset

1. Introduction

The San Francisco Public Utilities Commission's (SFPUC) Hetch Hetchy Regional Water System supplies an average of 260 million gallons of drinking water to 2.5 million people in the San Francisco Bay Area each day. The system was built in the early 1900s and carries water 267 km across California from the Hetch Hetchy Reservoir in Yosemite National Park to the Bay Area through a gravity-driven network of pipelines, tunnels, pump stations, dams, reservoirs and tanks as shown in Figure 1. Beginning in the city of Fremont, the water is conveyed in four pipelines, namely, Bay Division Pipelines (BDPLs) Nos. 1–4. BDPLs 1 and 2 carry the water westward across the San Francisco Bay, whereas BDPLs 3 and 4 turn southward and continue around the southern portion of the San Francisco Bay through Santa Clara and San Mateo counties.

BDPLs 3 and 4 are vital components of the SFPUC's water transmission system. One of the most vulnerable areas of the system is in the city of Fremont, where BDPLs 3 and 4 cross the Hayward Fault (Figure 1), an active fault with a significant probability of a large ground-rupturing earthquake. The most serious damage to underground pipelines during an earthquake has long been recognised as caused by permanent ground deformation (PGD) (Hamada & O'Rourke, 1992; O'Rourke, 1998; O'Rourke & Liu, 1999). One of the prominent PGD hazards is due to

fault rupture. Therefore, a new BDPL 3X is designed to replace the existing BDPL 3, and accommodate the design fault displacement. The new pipeline is designed to withstand a major earthquake and protect the pipe. The design entails enclosing BDPL 3X in a segmental reinforced concrete vault with special joints that can accommodate lateral offset and compressive deformation during fault rupture; the rotation and compression of the pipeline inside the vault are accommodated by ball joints and slip joints, respectively. However, the feasibility of this BDPL 3X system to accommodate fault rupture requires a detailed technical evaluation because it involves a complex mechanism of soil–structure interaction.

Different approaches have been applied to explore the soil–structure interaction behaviour of pipeline response to fault rupture. Trifonov and Cherniy (2012) presented an analytical model of the stress–strain analysis of buried steel pipelines subjected to active fault displacements. Simplified finite element methods (Cocchetti, di Prisco, & Galli., 2008; Joshi, Prashant, Deb, & Jain, 2011), which utilised beam elements for the pipeline and discrete nonlinear springs for the soil, have been commonly adopted to analyse buried pipelines subjected to fault motion in engineering practice. The complex soil–pipeline system can be rigorously modelled with 3D finite elements (e.g. Vazouras, Karamanos, & Dakoulas, 2010;

*Corresponding author. Email: tsaicc@nchu.edu.tw

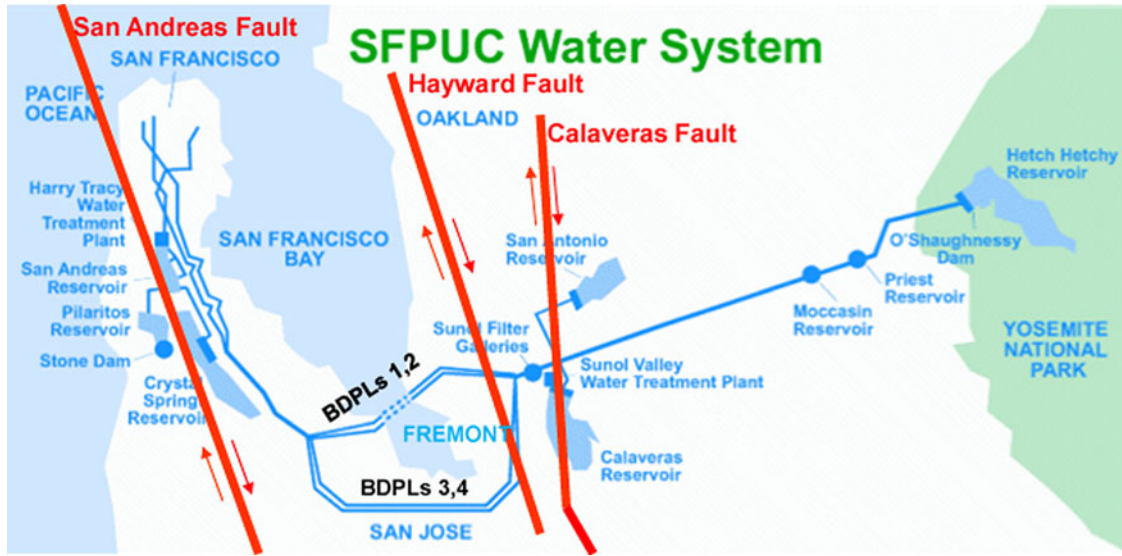


Figure 1. Hetch Hetchy regional water system and fault systems in the San Francisco Bay area.

Xie et al., 2013) to account for large strains and displacements, nonlinear material behaviour and special conditions of contact and friction on the soil–pipe interface. Large-scale (Kim et al., 2009; O'Rourke & Bonneau, 2007) and centrifuge tests (Ha et al., 2008; Moradi, Rojhani, Galandarzadeh, & Takada, 2013; O'Rourke, Gadicherla, & Abdoun, 2005) have also been employed to simulate the pipeline response to ground rupture and obtain the soil pressure distributions and lateral reaction of pipelines subjected to fault movement. However, most of these studies except for Kim et al. (2009) were conducted for continuous pipeline systems in response to fault ruptures. A segmented system, such as BDPL 3X, has been investigated.

Numerical analyses were performed in this study using the FLAC 3D finite difference model to better understand the behaviour of the BDPL 3X segmented vault subjected to fault rupture. In contrast to previous studies that focused on continuous pipelines, the present study emphasised the behaviour of segmented vaults that consist of reinforced concrete trapezoidal boxes with gaps between each segment. Different models were applied to explore the effect of fault position, backfill properties, native soil properties and connection joint sizes on the performance of the segmented vault.

2. Fault crossing design detail

2.1 Design basis

BDPL 3X crosses the Hayward Fault at approximately 47° (William Lettis and Associates [WLA], 2008), such that a right lateral strike-slip movement of the fault will cause compression in the pipeline. Strain limits are typically

utilised to guard against localised wrinkling or tensile fracture of the pipeline induced by PGD (American Lifelines Alliance [ALA], 2001a). The latest American Society of Civil Engineers (ASCE) Manual of Practice 119 for Buried Steel Pipes (ASCE, 2009) specifies the maximum allowable strain for compression equal to the minimum of $[0.01, 0.4t/D]$, in which t/D is thickness-to-diameter ratio of pipeline. Accordingly, steel pipes may sometimes be able to accommodate fault crossing displacements up to a few feet (ALA, 2001b) depending on compression strain that is dependent on fault-cross angle, fault deformation, surrounding soil strength, soil stiffness and pipeline properties.

Vazouras et al. (2010) recently presented design diagrams that depict critical fault displacement and the corresponding critical strain versus the pipe diameter-to-thickness ratio for various soil and pipeline parameters. According to Vazouras et al. (2010), given the site condition and the pipe properties of BDPL 3X, critical fault displacement is estimated to be approximately 2 ft (0.6 m), which is far below the design displacement of 6.5 ft (2.0 m). A special design solution is therefore required to prevent pipe failure.

2.2 Protective vault

To accommodate strike-slip offset in compression and protect the pipeline from wrinkling, the pipeline will be constructed in a protective segmental concrete vault at the fault crossing. The design concept is shown in Figure 2. Fault deformation or fault-induced compression strain can be accommodated by the relative slip and rotation of the connection joints. The length of the protective vault is ~ 91.4 m (300 ft), and the width, height and length of the reinforced concrete segments (boxes) are approximately 6.1 m (20 ft). The connection joints with 15-cm (6 in.)

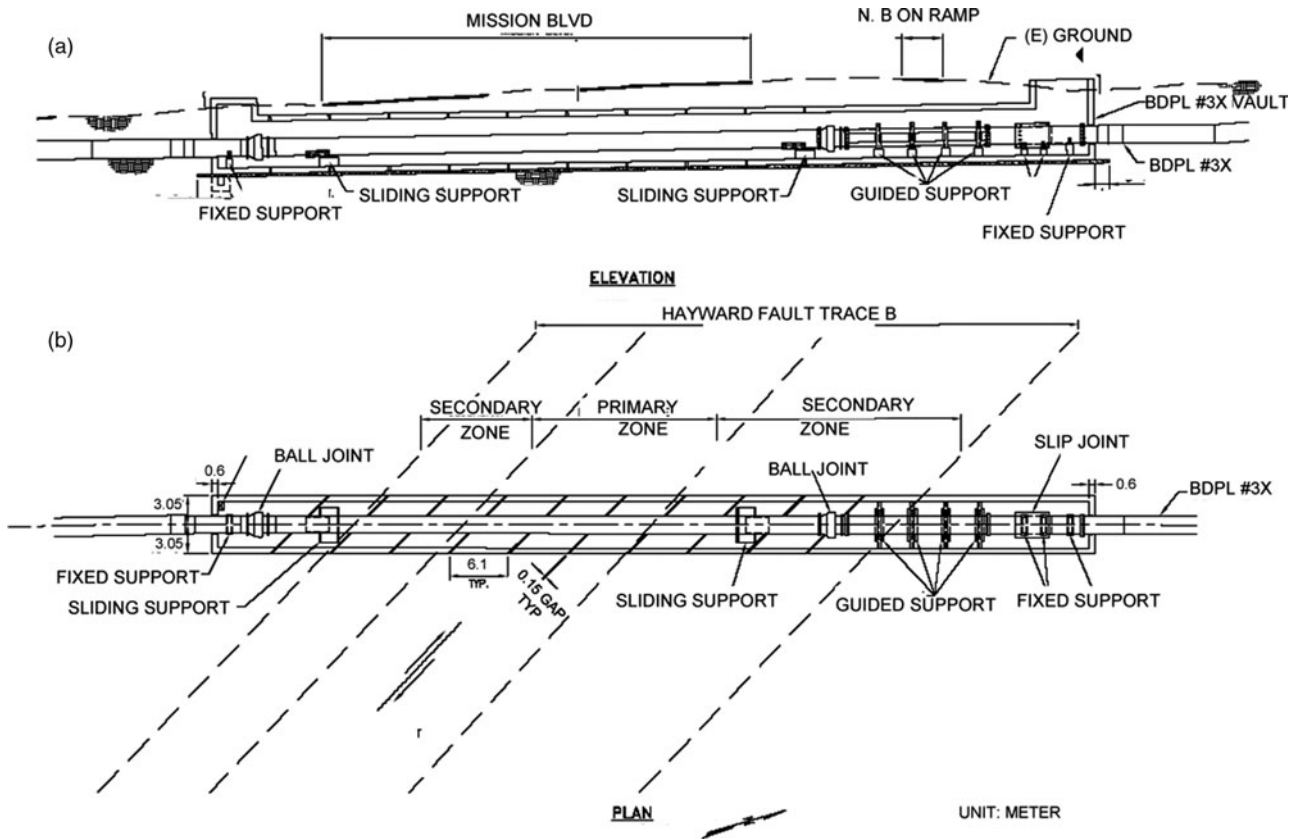


Figure 2. Design solution of BDPL 3X at the Hayward Fault crossing. (a) Section view along the pipeline longitudinal direction. (b) Plan view.

spacing between concrete segments are oriented at 45° with respect to the longitudinal axis of the vault; thus, they are approximately parallel to the strike of the fault. Figure 2 shows the ball joints installed in the pipeline to allow for rotation in response to a fault offset. A slip joint is installed to accommodate compression in the pipeline. The pipeline is supported by sliding and guided supports to allow and further control the horizontal movement. The protected vault segments are cast in place on unreinforced mud slabs.

2.3 Shoring system

The newly designed BDPL 3X will be constructed by top-down construction method and will carry a series of temporary bridges to carry traffic across Mission Boulevard and the northbound Interstate 680 on-ramp north of Mission Boulevard. The depth of excavation will be approximately 9 m. The excavation shoring system is designed as two parallel cast-in-drilled-hole (CIDH) secant pile walls that consist of a series of overlapping primary and secondary piles. The short primary piles are constructed with lean concrete, and the long secondary piles are constructed with reinforcing cages and structural concrete.

The CIDH wall will remain in place after the vault is constructed. A typical completed section after the upgrade, as shown in Figure 3, includes the protective vault, bottom mud slab, secant pile wall, backfill between the vault and secant pile wall and compacted pavement and subgrade. The presence of the CIDH wall and other components can also affect the vault response during fault movement.

3. Numerical analysis

Three-dimensional (3D) numerical analyses of the soil-structure interaction were performed to gain insight into the behaviour of BDPL 3X in response to a fault rupture. A critical aspect of the system is the relative movement of the concrete vault segments to accommodate lateral offset and compressive deformation during fault rupture. Understanding the relative movement of the segments with respect to one another and the effects on the enclosed pipeline (i.e. rattle space, the distance between the pipeline and the vault wall) is a key component of the investigation process. Therefore, analyses were performed to focus on the behaviour of the segmental concrete vault. The entire pipeline and its supports were not included in the numerical model.

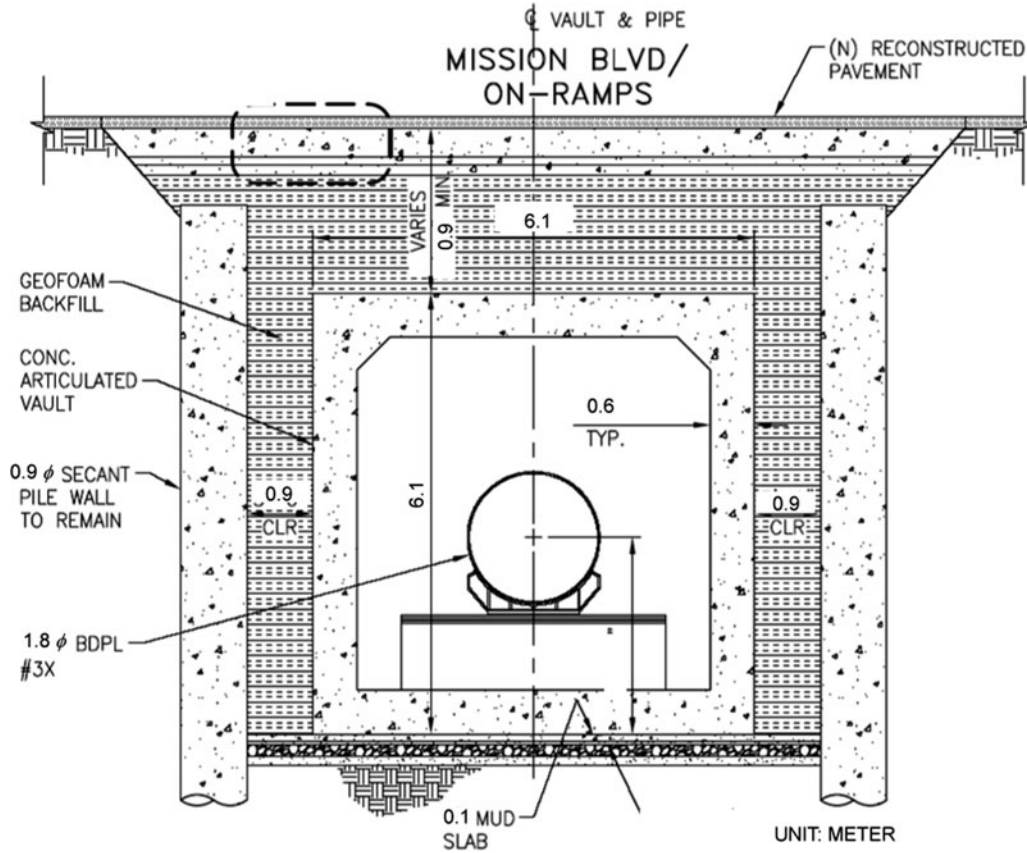


Figure 3. Cross section along the pipeline transverse direction.

3.1 FLAC 3D model

The FLAC 3D model captures the primary design features (Figure 3), including the vaults, secant pile wall (primary and secondary piles), bottom mud slab, native soil, backfill and compacted fill (pavement subgrade), and has a total of 50,000 elements. Figure 4 shows the overall view of the model mesh. Fine meshes were generated near the fault (centre of the model) and pipeline alignment. To accommodate a 45° vault angle and a 45° – 50° fault intersection angle, all meshes were generated in a ‘parallelogram’ shape by using the selected angle with respect to the pipeline transverse direction. The purpose of this setup is not only for convenience in mesh generation but also to avoid significant distortion in the elements when the model encounters a large fault displacement. Another feature of the model (as shown in Figure 5) includes the connection joints (gaps) between vaults, which also impose challenges in mesh generation and computation stability owing to their small size compared with the entire model. Furthermore, interface elements were installed on all surrounding vaults to allow for relative movements between the vault segments (boxes) and the surrounding elements and to monitor the contact forces if the boxes collide. The nine vault segments (boxes) closest to the fault

rupture plane were modelled to understand the box reactions relative to the fault trace.

The different model types and the corresponding properties assigned to the different materials are listed in Table 1. The segmented vaults were modelled as rigid boxes because the primary purpose of the simulation is to understand the global behaviour of the vaults. The connection joints between the segment vaults were reproduced by a null model that induces zero stiffness. The secant pile walls that consist of a series of primary and secondary piles were modelled by a composite of solid and pile elements. Short primary piles without reinforcement were built with solid elements with a size that produces equivalent bending stiffness. A strain softening model was adopted to capture the weakening behaviour of the primary pile (i.e. a fault could rupture through). Meanwhile, long reinforced piles were simulated with a composite of structure pile and solid elements with a size that produces equivalent bending stiffness. Mud slabs without reinforcement were also established by the strain softening model similar to that of the primary pile of the secant pile wall. Geof foam backfill, which exhibits strain hardening behaviour, was modelled by a double-yield model with calibrated model parameters.

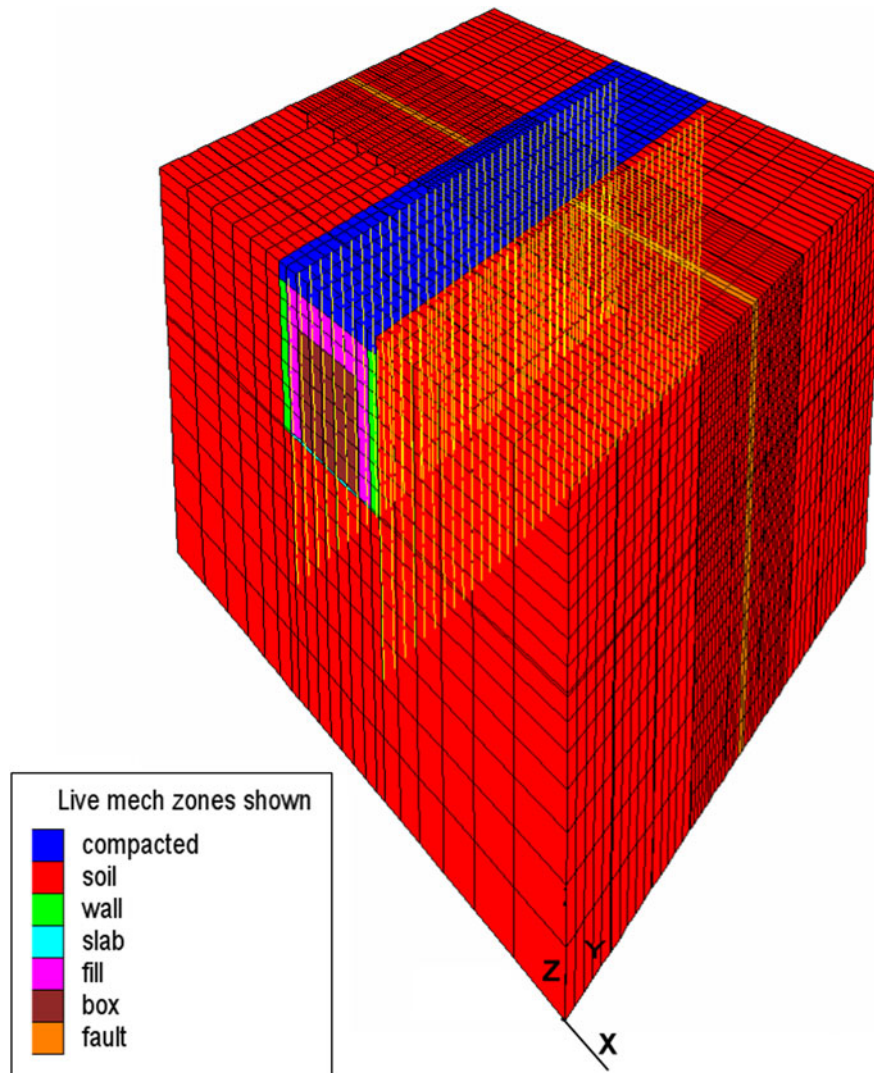


Figure 4. FLAC 3D model and 3D view.

3.2 Boundary condition and analysis procedure

Prior to the fault rupture simulation, the gravity load was applied first so that the model could achieve equilibrium condition. At this stage, the bottom of the model was designated with fixed boundary conditions (translations of three directions were prevented), whereas the four sides were fixed in the horizontal direction but remained free in the vertical direction. No staged construction in the excavation, such as secant pile wall installation and vault placement, was modelled. In the second stage, the boundaries on the four sides and bottom of the model were fixed in the three directions and then subjected to displacements similar to those of a rigid shear box movement to mimic a fault rupture.

The models were simulated to impose a straight, planar (knife edge) ground rupture without dispersion of the fault trace to set an upper bound for the deformation effects.

Half of the design fault displacements (1.0 m) were applied incrementally at each side of the fault plane in opposite directions rather than impose the entire design fault displacement (2.0 m) on one side so that the model could attain equilibrium faster. The analysis was conducted under a quasi-static condition, which applies fault offset gradually to allow the model to reach equilibrium at each incremental fault movement.

3.3 Analysis output

When the fault displacements were applied, the model continuously monitored the movement of the boxes and the forces that act on the boxes induced by the fault movement. Figure 6 shows the notation of output data related to box mobility, including the box rotations along the longitudinal, transverse and vertical directions, the two

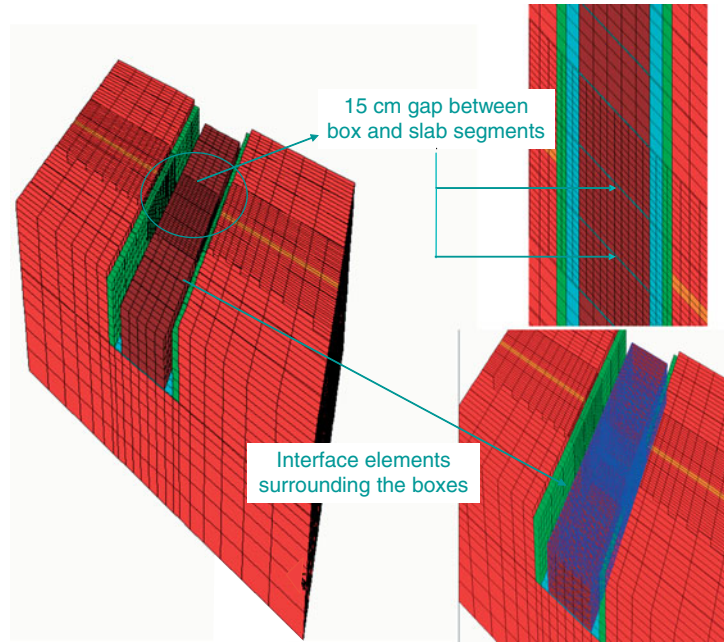


Figure 5. Features of the FLAC 3D model: 15-cm gaps and the surrounding interface elements outside the boxes.

Table 1. Models and parameters utilised in FLAC analysis.

Material	Model	Parameter
Native soil (lower bound)	Mohr–Coulomb	S_u (Table 3), $E = 250 S_u^a$, $\nu = 0.5$, $\gamma = 19.7 \text{ kN/m}^3$
Native soil (upper bound)	Mohr–Coulomb	S_u (Table 3), $E = 600 S_u^b$, $\nu = 0.5$, $\gamma = 19.7 \text{ kN/m}^3$
Loose sand backfill	Mohr–Coulomb	$c' = 0$, $\phi = 30$, $E = 13.8 \text{ MPa}$, $\nu = 0.2$, $\gamma = 18.9 \text{ kN/m}^3$
Geofoam backfill	Double yield	$q_u = 23.4 \text{ kPa}$, $E = 2.39 \text{ MPa}$, $\nu = 0.08$, $\gamma = 0.14 \text{ kN/m}^3$
Compacted fill	Mohr–Coulomb	$c' = 0$, $\phi = 36$, $E = 68.8 \text{ MPa}$, $\nu = 0.35$, $\gamma = 20.4 \text{ kN/m}^3$
Box	Elastic	$E = 27,000 \text{ MPa}$, $\nu = 0.18$, $\gamma = 23.6 \text{ kN/m}^3$
Slab	Strain softening	$f_c^t = 332 \text{ MPa}$, $E = 8260 \text{ MPa}$, $\nu = 0.18$, $\gamma = 22.8 \text{ kN/m}^3$
Primary pile of the secant pile wall	Strain softening	$f_c^t = 332 \text{ MPa}$, $E = 8260 \text{ MPa}$, $\nu = 0.18$, $\gamma = 22.8 \text{ kN/m}^3$
Secondary pile of the secant pile wall	Beam	$E = 23,800 \text{ MPa}$, $\nu = 0.18$, $\gamma = 23.6 \text{ kN/m}^3$
Gap	Null	–

^a Assuming that $\text{OCR} = 2$ and $\text{PI} = 50$ (Duncan & Buchignani, 1976).

^b Assuming that $\text{OCR} = 2$ and $\text{PI} = 30$ (Duncan & Buchignani, 1976).

sides of the box offset (east and west) relative to the adjacent box and the gap spacing. The forces that act on the boxes, including normal forces acting on the two sides of the box and box-to-box contact forces, were also monitored.

3.4 Analysis cases

Ten cases, presented in Table 2, were analysed. The analysis of these cases was performed in consideration of the factors that can affect box movement, including fault location, fault angle, native soil strength, backfill type and connection joint size. Case 1 was utilised to evaluate the effect of fault location on box movement. The fault plane was made to pass through the centre, the quarter point and the edge of the central box. Case 1-A, which utilised the

best estimated model parameters (47° of the fault angle, lower bound of the soil strength and sand backfill) was defined as the baseline model. Case 2 was utilised to evaluate the effect of the fault angles on box movement. According to the range of fault angles reported by WLA (2008), the analysed fault angles were set to 45° and 50° in Cases 2-A and 2-B, respectively.

Case 3 was utilised to evaluate the effect of variation in native soil strength (medium to very stiff clays as listed in Table 3 according to URS Corporation [2010]) and backfill type on box movement. In Case 3-A, the upper bound native soil strength was adopted; the other variables were kept similar to those of the baseline model. In Case 3-B, a Geofoam-type backfill was utilised; however, the other variables were kept similar to those of the baseline model. Case 4 was utilised to evaluate the impact of

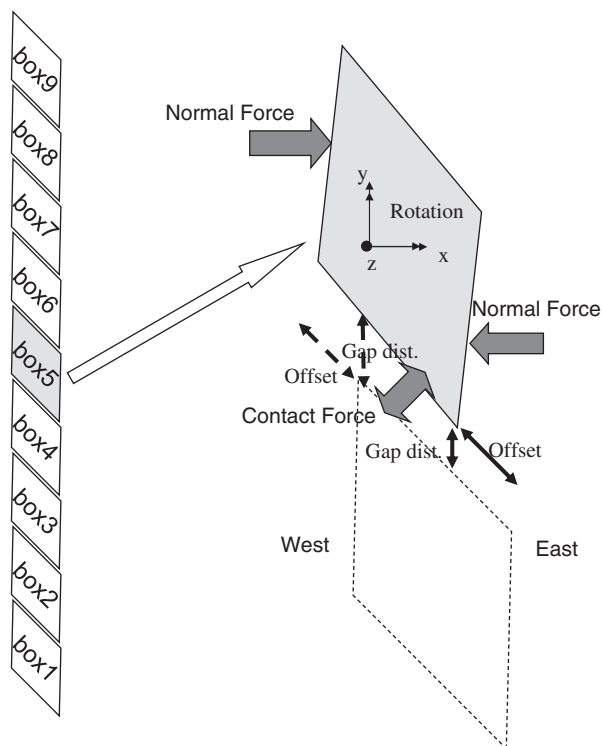


Figure 6. Notation of the output parameters.

connection joint size on box movement. In addition to varying the connection joint size from 6 in (15 cm) to 12 in (30 cm), the other analysed variables were selected based on the results of Cases 1–3 to consider the most unfavourable condition.

4. Model verification with a large-scale test

The modelling technique described previously was verified against physical model data obtained from a large-scale test. The 1/10 scale models of the protective concrete enclosures were established with the Large-Scale Lifelines Testing Facility at Cornell University, which is a part of the Network for Earthquake Engineering Research.

Table 2. FLAC analysis cases.

Case	Fault location	Fault angle (°)	Box angle (°)	Joint size (cm)	Soil strength	Backfill	Note
1-A	Centre of the box	47	45	15	Lower bound	Sand	Baseline model
1-B	Quarter of the box	47	45	15	Lower bound	Sand	
1-C	Edge of the box	47	45	15	Lower bound	Sand	
2-A	Centre of the box	45	45	15	Lower bound	Sand	
2-B	Centre of the box	50	45	15	Lower bound	Sand	
3-A	Centre of the box	47	45	15	Upper bound	Sand	
3-B	Centre of the box	47	45	15	Lower bound	Geofoam	
4-A	Quarter of the box	50	45	15	Upper bound	Geofoam	
4-B	Quarter of the box	50	45	22.5	Upper bound	Geofoam	
4-C	Quarter of the box	50	45	30	Upper bound	Geofoam	

Similar to the purpose of FLAC analysis, the scale model tests also aim to validate the effect of fault location and back fill type on box movement. However, unlike FLAC analysis which considered a range of fault angles, the fault angles of the Cornell scale model tests were fixed at 50°. In addition, the constraints of the cover plate between connection joints were varied in these tests, unlike the FLAC analysis. The details of the Cornell model test can be obtained from Cornell University (2009).

FLAC Case 4-C and Cornell Case 1-E, designed for similar scenarios, were selected for comparison. The verification focused on the generalised relative displacement of the boxes caused by fault movement, specifically, the relative offset and rotation of the boxes. Figure 7 shows the comparison of FLAC simulation results and the Cornell model test results. The lateral displacements of the vault segments shown in Figure 7(d) are relative to a horizontal line that represents the initial position of the south end vault before fault rupture. The Cornell test reported the movement of the centre of box, whereas FLAC reported the movement of the four corners of the box. It is easier to observe the offset between two adjacent boxes. The FLAC simulation of box response agrees favourably with that of the Cornell model test in terms of rotations and lateral displacements.

5. Soil–structure interaction behaviour

The BDPL 3X system will interact with the surrounding soil (referred to as soil–structure interaction) and cause the ground rupture to behave differently. Figure 8 shows the displacement contour at a 2.0-m fault displacement of Case 4-A. In the bottom view where only the soil is shown,

Table 3. Soil strength profile (URS, 2010).

Depth (m)	Lower bound S_u (kPa)	Upper bound S_u (kPa)
0–9	140–40	360–275
9–12	41	275
12–21	40–230	275–360
21–33	40	360

Note: S_u linearly changes with depth if a range of S_u is presented

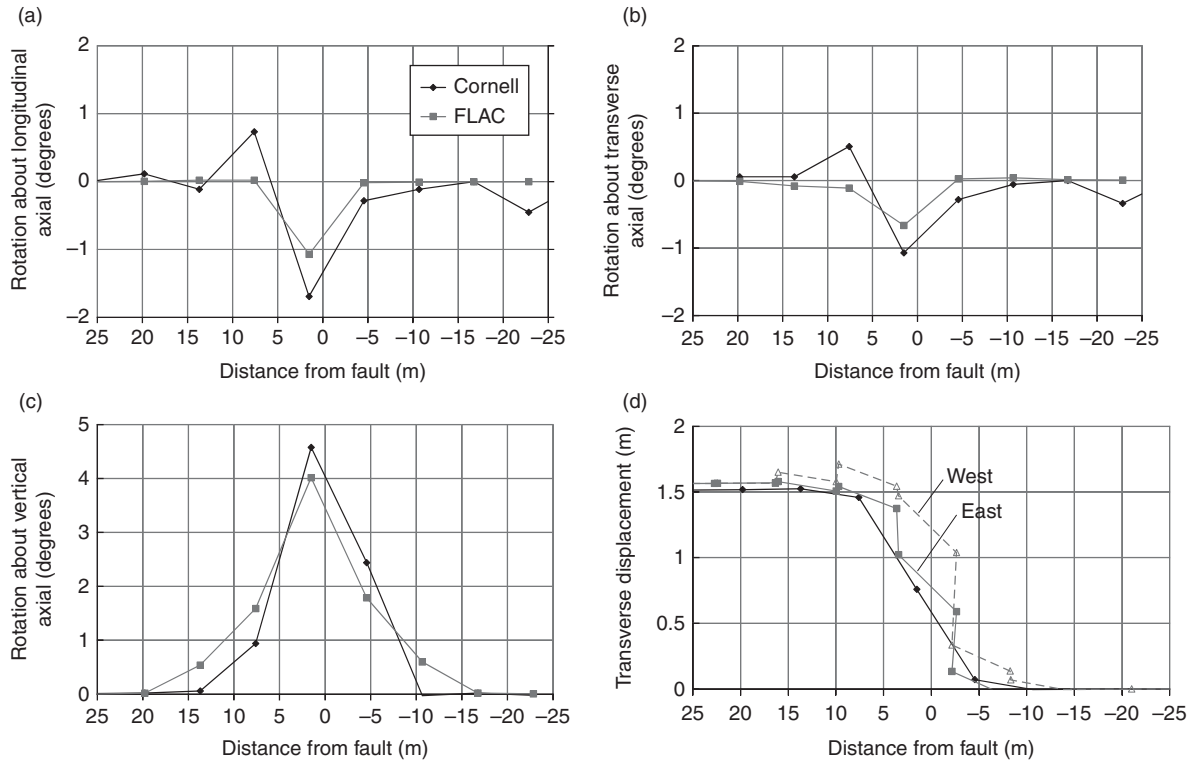


Figure 7. Comparison of FLAC simulation results and Cornell model test results.

a knife-edge type of fault displacement is clearly observed because the models were simulated by introducing a straight planar ground rupture. The top view, however, shows that the fault movement spreads out because of the interference of the BDPL 3X system. Moreover, the cut

section view near the fault plane indicates that different displacements of the adjacent native soil are developed.

The soil deformed upon contact with the system in opposite directions from each side of the fault in response to the right lateral strike-slip displacement. This condition typically generates a passive pressure reaction at each side of the fault as shown in Figure 9. The soil on the other sides of the vault opposite the passive pressure sides tended to move away from the concrete segments and thus created an active pressure zone as shown in Figure 9. These phenomena are consistent with those in a previous study on continuous systems (O'Rourke et al., 2008). However, soil zones (active and passive) in Figure 9 exhibit different apparent sizes on the different sides of the system. This is because the fault plane was made to pass through the quarter point of box, which imposes a non-symmetric condition.

The active pressure or extension zones are confined to the region bounded by a distance of approximately 1–1.5 segment lengths from either side of the fault. The system has a limited capability to transfer the bending stresses and distribute the axial compression induced by the fault offset because of the weak connection joint between the boxes opposite the continuous pipeline. Consequently, major soil structure interaction is encountered within a narrow region.

Figure 10 depicts the plan view of the deformed mesh 6.1 m below the ground surface (mid elevation of the box)

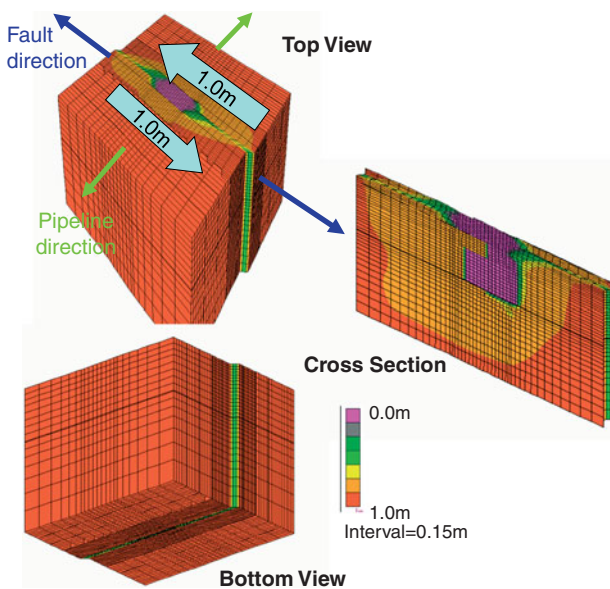


Figure 8. 3D view of the displacement contour, Case 4-A.

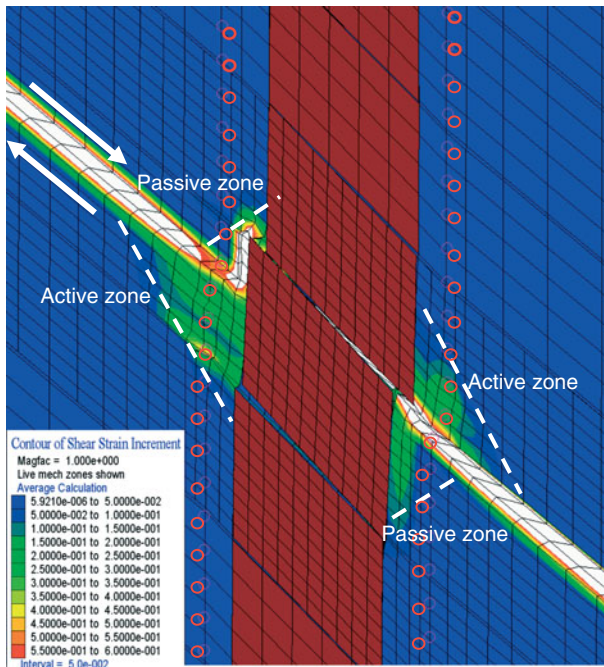


Figure 9. Plan view of the shear strain contour 6.10 m below the ground surface at a 2.0-m fault movement, Case 4-A. The circles indicate the secondary pile location.

after a 2.0-m fault displacement. Some of the observed general features of the system response are as follows:

- The boxes experienced rotation and lateral movement (offset) as rigid bodies.
- Some gaps were closed (i.e. boxes collided) as a result of box rotation and lateral offset. Partial connection joint closure occurred as far as one to two segments from both sides of the fault.
- The space between the vault and the secant pile wall was reduced at one side (points A and A' where the fault moved toward the vault) and widened at the other side (points B and B' where the fault moved away from the vault).
- The fault rupture broke through the secant pile wall at the location of the unreinforced primary pile. Consequently, soil displacement propagated through this weak point and imposed lateral offset on the segmented vaults at the connection joints.

6. Monitored analysis output

The history of the box mobility subjected to fault offset can be better understood by continuously monitoring with FLAC. Figure 11 shows an example of the monitored data of Case 4-A on box rotation, box offset, gap distance, side force acting on the box and box-to-box contact forces corresponding to different fault displace-

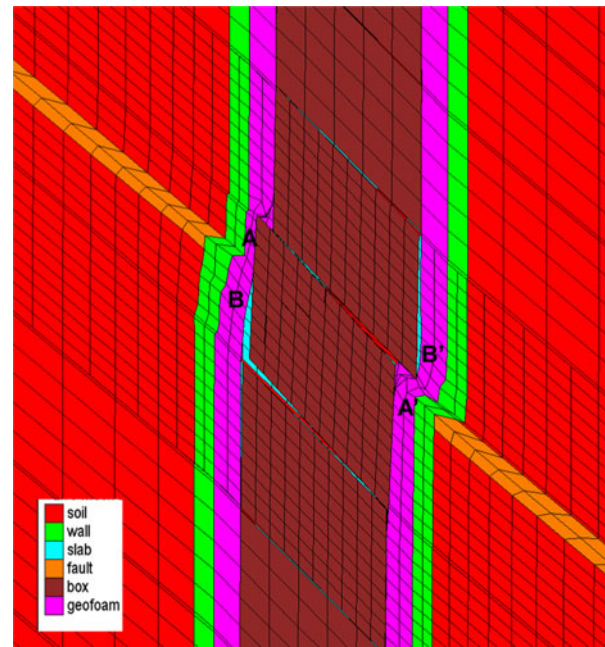


Figure 10. Plan view of the deformed mesh 6.1 m below the ground surface (middle elevation of the boxes) at a 2.0-m fault movement, Case 4-A.

ments. The system response can be further characterised as follows:

1. The boxes experienced rotation. The box rotation along the vertical axis at the centre box (Box 5) increased linearly (starting at 0.1 m fault offset) with the fault movement up to 2.7° at a 2.0-m fault displacement. The two adjacent boxes exhibited delayed responses (starting at 0.5 m fault offset) and rotated linearly initially up to a 1-m fault offset before reaching the maximum rotation at the 1.1-m fault displacement. The boxes also exhibited rotation along the transverse and longitudinal axes; however, such rotation was insignificant compared with the rotation along the vertical axis.
2. The boxes moved laterally. The degree of translation can be quantified by the offset between two adjacent boxes as indicated in Figure 6. The box offset at the centre increased linearly with the fault movement and reached 1.1 m at a 2.0-m fault displacement. Similar to the rotation response, the offset mostly occurred near the fault trace.
3. The combined effects of rotation and translation (both longitudinal and transverse directions) were reflected in the reduced or opened gap width. In this case, the gap between Boxes 4 and 5 began to close at the 0.6-m fault displacement on one side, whereas the gap on the other side tended to widen. The gaps between Boxes 3 and 4 and between Boxes 5 and 6 closed eventually at the 0.9-m and

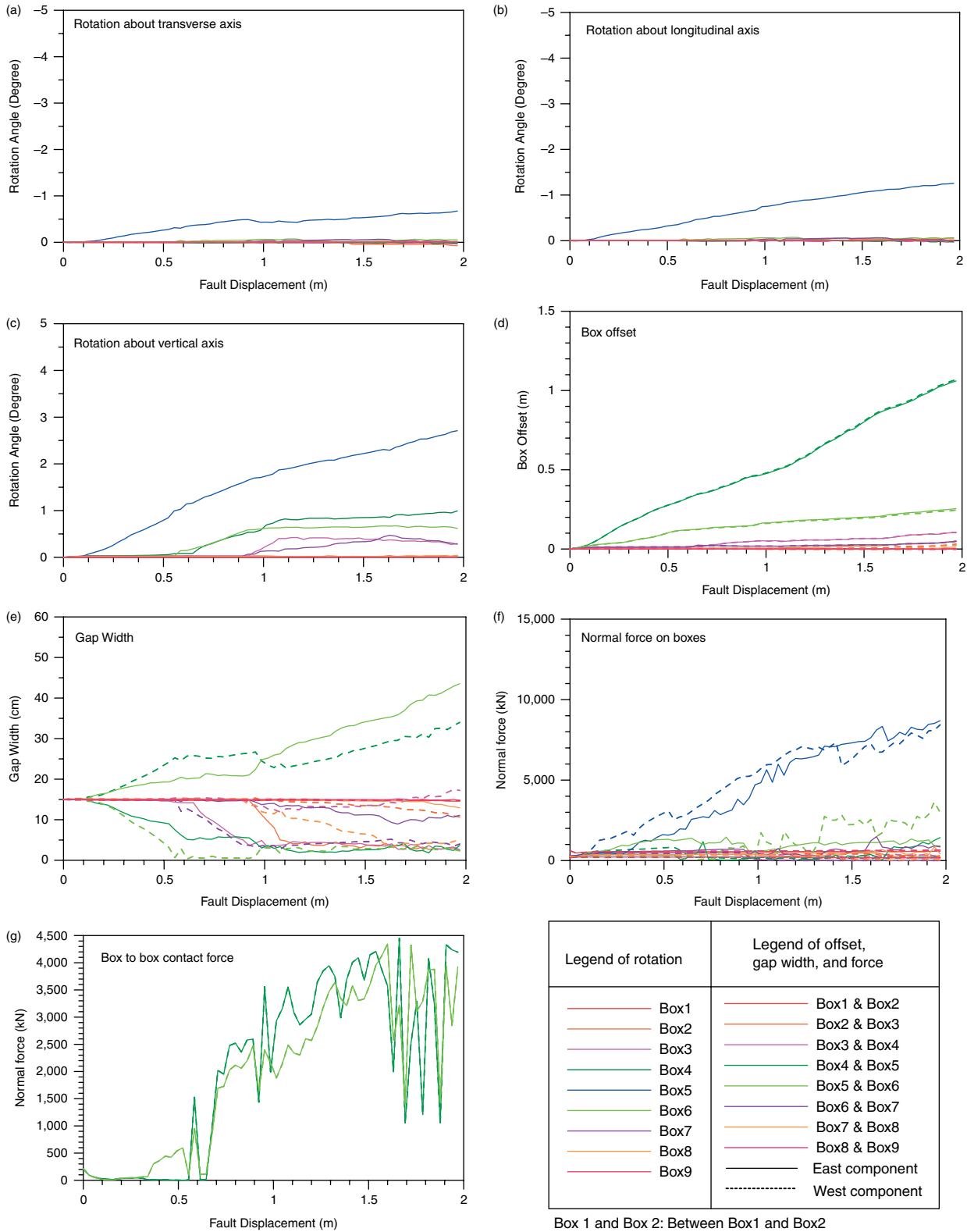


Figure 11. Box response versus fault movement, Case 4-A.

Downloaded by [122.118.5.156] at 19:32 10 October 2014

1.1-m fault displacements, respectively. Right lateral fault movement with an approximate 45° intersection angle imposes a compression mode to the system and reduce gap width typically. However, the fault movement also cause the box rotation, which can increase or decrease gap size on each side of box depending on the magnitude of box rotation relative to the adjacent one. The centre box experienced largest rotation to overcome the compression and, thus, resulted in gap opening while the other gaps showed closing.

4. According to items 1–3, box deformation as indicated by the box rotation, box offset and gap distance occurred primarily within the central three boxes near the fault trace.
5. At approximately the 0.5-m fault movement, the model began to detect the box-to-box contact force, which is also the moment when the gap closed.
6. The normal stress on the side wall of the boxes increased with fault displacement. The increase in stress was due to the passive pressure transmitted to the backfill material between the box and the secant pile wall as shown in Figure 9. Unlike box deformation, however, the increase in stress occurred primarily at the centre box.

7. Variations in vault response

The variations in fault location, fault angle, material strength and connection joint size were considered from Cases 1-A to 4-C and were implemented in the FLAC model to evaluate the effect of these factors on system response. Figure 12 shows the final box position under the 2.0-m fault movement. Figure 13 provides a comparison of the responses of the different cases. As shown in Figure 13, the forces acting on the box are normalised by the maximum horizontal passive pressure mobilised by the native soil. The analysis results are discussed below:

1. Case 1 – Variation in the fault location: The maximum box rotation about vertical axis occurred in the case where the fault was forced to rupture at the quarter point of the box, and the largest box offsets (i.e. greatest reduction in the rattle space) were observed with the fault at the edge of the box. However, the fault movement-induced soil force was similar regardless of the fault location.
2. Case 2 – Variation in the fault angle: Comparison of Cases 1-A, 2-A and 2-B indicates that the maximum box rotation occurred at a fault intersection angle of 50° , which is the maximum difference between the fault and the box angles. The box rotation in this case was considerably higher than that in the other two cases; consequently, the gap space closed at the 1.5-m fault movement. Moreover, the fault movement-induced soil force in this case was also higher than in the other two cases.
3. Case 3 – Variation in the materials: In the high stiffness contrast between the native soil and the backfill material (e.g. Case 3-A vs. Case 1-A or Case 1-A vs. Case 3-B), more box rotations but less box offsets were achieved. In this condition, box mobility presented a wider range of distribution but a more general deformed shape along the longitudinal direction as shown in Figure 12. The highest forces were measured in the boxes with upper bound native soil strength, and the lowest forces were measured in the boxes with Geofom backfill.
4. Case 4 – Variation in the gap size: Case 4-A–C were set up to promote maximum rotation with the following conditions: the fault is aligned at the quarter point of the box, fault angle of 50° and high stiffness contrast between the native soil and the backfill material. A large gap width results in large box rotation but small offset. However, the net result is similar in terms of rattle space as shown in Figure 13 (f). Different gap widths result in similar box-to-box contact forces and normal forces acting on the boxes.

All analyses showed relatively low levels of vertical segment movement and rotation in the lateral and longitudinal axes of the vault. The rotations about the vertical axis (on the horizontal plane) were significant but still distributed only within one to two segments on either side of the fault. Hence, the box rotations on the horizontal plane are extremely important for the proper functioning of the pipeline inside the vault. The deformation of the vault on the horizontal plane was affected by the following: (1) location of the fault as either centred on a segment or centred on a connection joint and (2) nature of the backfill between the vault and the secant pile wall.

The narrowest distribution of the segment movements (combination of translation and rotation) from the fault plane, which conforms to the most pronounced deformation of the vault, occurred when the connection joint was centred on the fault. The widest distribution of the segment movements from the fault plane, which conforms to the most gradual deformation of the vault, occurred when the segment was located on the fault. The use of Geofom as backfill increased the maximum segment rotation and broadened the distribution of the rotation compared with the use of loose sand as backfill. Lastly, the variation in the connection joint size in a narrow range has a minimal impact on the mobility of the box in response to fault rupture.

The highest lateral pressure on the vault segments was measured in cases where loose sand was placed between the vault and the secant pile wall. The highest pressure associated with the fault was approximately 30% of the maximum horizontal passive pressure. The lowest horizontal pressure was measured in cases where Geofom

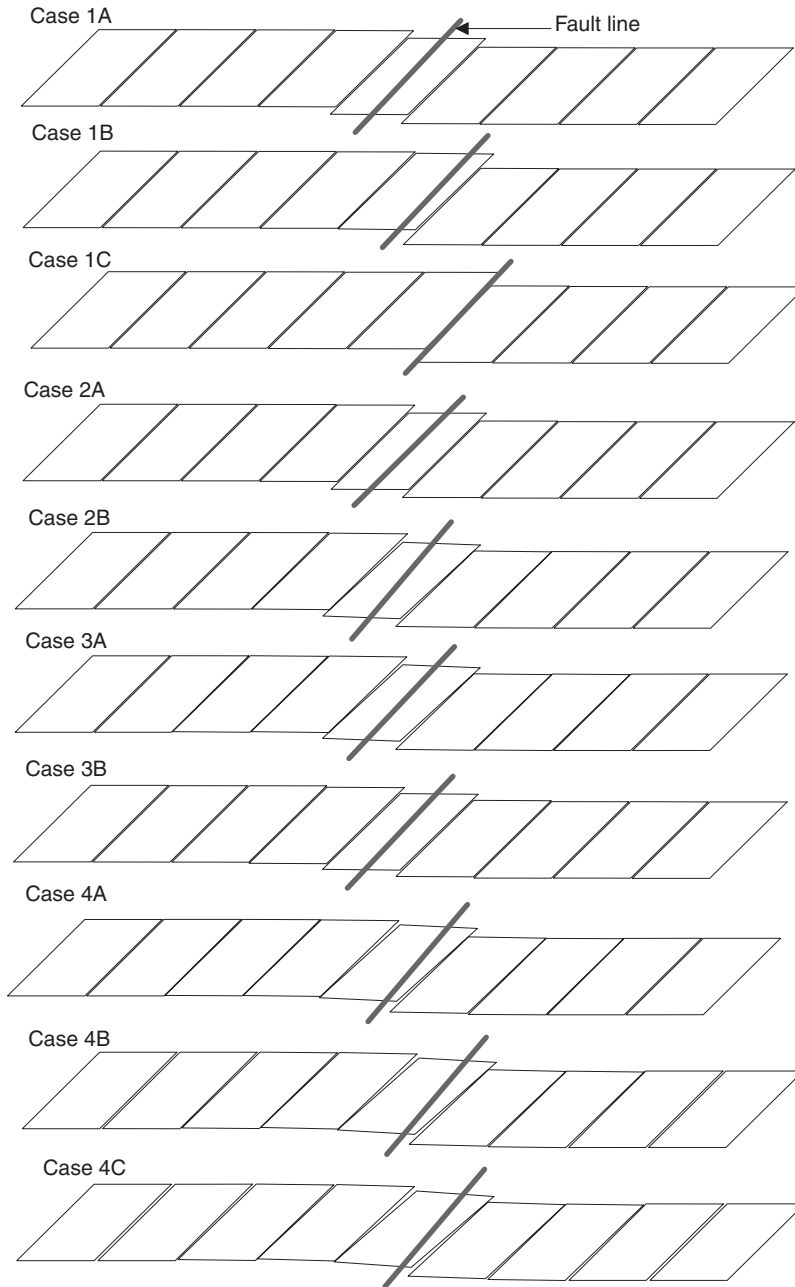


Figure 12. Final box positions at a 2.0-m fault displacement for the different cases.

was utilised as back fill. The pressure in these cases was equal to or less than 10% of the maximum horizontal passive pressure and less than 30% of the mobilised lateral pressure when loose sand was placed between the vault and the secant pile wall. The relatively low measured pressure compared with the maximum passive limits observed in the model simulation results from the secant pile wall, which acts as a barrier between the vault and the soil on the outboard side of the wall. During a fault rupture, soil movement is resisted by the secant pile wall, resulting in shear transfer between the soil and the intact

structural wall elements. This interaction between the deformed soil and the secant pile wall reduces the pressure transmitted to the vault to a relatively small fraction of the maximum horizontal passive pressure.

8. Summary and conclusions

The seismic upgrade of BDPL 3 and 4 involves the replacement of the existing BDPL 3 with a new BDPL 3X enclosed in a segmental protective vault at its crossing of the Hayward Fault. Numerical 3D model analyses were

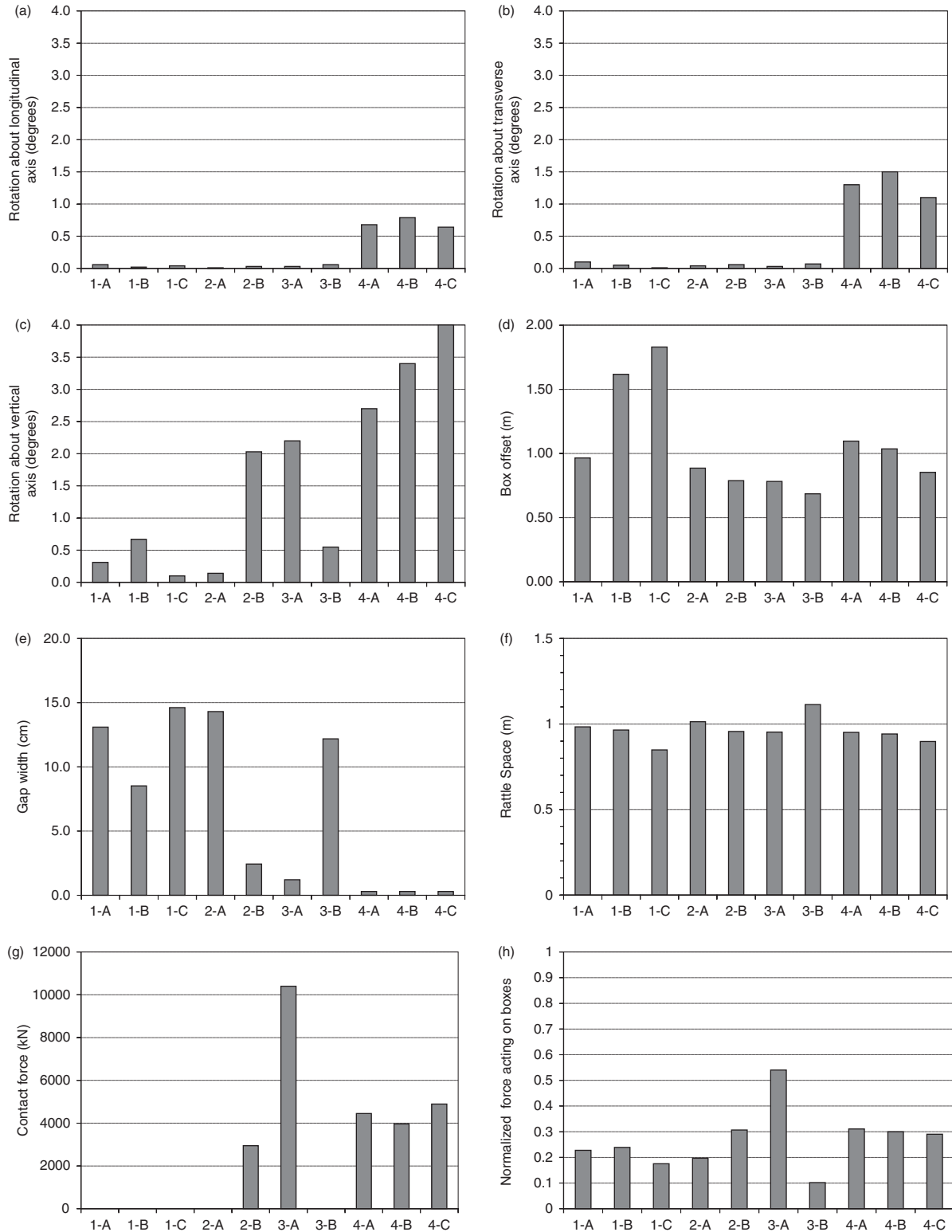


Figure 13. Comparison of the output parameters at a 2.0-m fault displacement for the different cases.

performed to simulate the complex protective vault system when subjected to fault rupture. The analyses provide information on the relative movement of the segments,

including rotation, relative offset and induced forces, and thus enhances the understanding of the interaction among the concrete vault, backfill and native soil.

The influencing factors, such as fault location, fault angle, fill material type and native soil condition were studied. In response to a fault rupture in general, the segmental vaults experienced rotation and translation as rigid bodies. As a result, the connection joints between the vaults partially closed as far as one to two segments from either side of the fault. The compressive shortening of the vault caused progressive closure of the connection joints, which spread further from the fault as the strike-slip displacement increased.

From the point of view of design, we recommend designing the vault angle closer to the fault angle so that box rotation as well as contact force can be minimised. The analyses also demonstrated that connection joint size has a minimal impact on system performance. Although a large connection joint size results in more box rotation but less box offset, the net result is similar in terms of rattle space at the design fault movement. Lastly, Geofoam fill can significantly reduce the earth pressure on the vault compared with sand fill and leads to a more gradual deformation along the longitudinal axis. Therefore, Geofoam is recommended for backfill.

Conclusively, the simulated vault deformation validated the special design of rigid concrete segments with relatively flexible connection joints oriented parallel to the strike of the fault. After a design level of fault offset, the deformed vault will leave enough rattle space for the pipeline to accommodate the fault offset with slip and rotation joints.

Funding

This study was mainly conducted by the first author during his employment with URS Corporation and completed with funding from the National Science Council [grant number NSC101-2218-E-005-005]. The authors gratefully acknowledge this support.

Notes

1. Email: philip.meymand@urs.com
2. Email: ethan.dawson@urs.com
3. Email: sawong@sflower.org

References

- American Lifelines Alliance (2001a). *Guideline for the design of buried steel pipeline*. Retrieved from <http://www.americanlifelinesalliance.com/pdf/Update061305.pdf>
- American Lifelines Alliance (2001b). *Seismic fragility formulations for water systems, Part 1 – Guideline*. Retrieved from http://www.americanlifelinesalliance.com/pdf/Part_1_Guideline.pdf
- American Society of Civil Engineers (2009). *Buried flexible steel pipe: Design and structural analysis*. Reston, Virginia: ASCE Manual of Practice.
- Cocchetti, G., di Prisco, C., & Galli, A. (2008). Soil-pipeline interaction along active fault systems. *International Journal of Offshore and Polar Engineering*, 18, 211–219.
- Cornell University (2009). *Large-scale testing of fault rupture effects*. Ithaca, NY: Report prepared for San Francisco Public Utilities Commission.
- Duncan, J.M., & Buchignani, A.L. (1976). *An engineering manual for settlement studies: Department of Civil Engineering*. Berkeley: University of California.
- Ha, D., Abdoun, T.H., O'Rourke, M.J., Symans, M.D., O'Rourke, T. D., Palmer, M.C., & Stewart, H.E. (2008). Centrifuge modeling of earthquake effects on buried high-density polyethylene (HDPE) pipelines crossing fault zones. *Journal of Geotechnical and Geoenvironmental Engineering*, 134, 1501–1515. doi: 10.1061/(asce)1090-0241(2008)134:10(1501)
- Hamada, M., & O'Rourke, T.D. (1992). *Case studies of liquefaction and lifeline performance during past earthquakes*. Buffalo, NY: National Center for Earthquake Engineering Research.
- Joshi, S., Prashant, A., Deb, A., & Jain, S.K. (2011). Analysis of buried pipelines subjected to reverse fault motion. *Soil Dynamics and Earthquake Engineering*, 31, 930–940. doi: 10.1016/j.soildyn.2011.02.003
- Kim, J., Lynch, J.P., Michalowski, R.L., Green, R.A., Pour-Ghaz, M., Weiss, W.J., & Bradshaw, A. (2009). *Experimental study on the behavior of segmented buried concrete pipelines subject to ground movements*. Paper presented at the nondestructive characterization for composite materials, aerospace engineering, civil infrastructure, and homeland security.
- Moradi, M., Rojhani, M., Galandarezadeh, A., & Takada, S. (2013). Centrifuge modeling of buried continuous pipelines subjected to normal faulting. *Earthquake Engineering and Engineering Vibration*, 12, 155–164. doi: 10.1007/s11803-013-0159-z
- O'Rourke, M.J., Gadicherla, V., & Abdoun, T. (2005). Centrifuge modeling of PGD response of buried pipe. *Journal of Earthquake Engineering and Engineering Vibration*, 4, 69–73.
- O'Rourke, M.J., & Liu, X. (1999). *Response of buried pipelines subject to earthquake effects*. Buffalo, NY: MCEER.
- O'Rourke, T.D. (1998). *An overview of geotechnical and lifeline earthquake engineering*. Paper presented at the geotechnical earthquake engineering and soil dynamics conference, Seattle, WA.
- O'Rourke, T.D., & Bonneau, A. (2007). Lifeline performance under extreme loading during earthquakes. In *Earthquake Geotechnical Engineering* (pp. 407–432). Dordrecht: Springer.
- O'Rourke, T.D., Palmer, M.C., Jezerski, J.M., Olson, N.A., Abdoun, T., Ha, D., & O'Rourke, M. (2008). *Geotechnics of pipeline system response to earthquakes*. Paper presented at the geotechnical earthquake engineering and soil dynamics IV, Sacramento, CA.
- Trifonov, O.V., & Cherniy, V.P. (2012). Elastoplastic stress–strain analysis of buried steel pipelines subjected to fault displacements with account for service loads. *Soil Dynamics and Earthquake Engineering*, 33, 54–62.
- URS Corporation (2010). *Bay division pipelines 3 & 4 Hayward fault crossing geotechnical report*. Report prepared for San Francisco Public Utilities Commission, Fremont, CA.
- Vazouras, P., Karamanos, S.A., & Dakoulas, P. (2010). Finite element analysis of buried steel pipelines under strike-slip fault displacements. *Soil Dynamics and Earthquake Engineering*, 30, 1361–1376. doi: 10.1016/j.soildyn.2010.06.011
- William Lettis and Associates (2008). Internal memo to URS on design criteria for the Hayward Fault movement.
- Xie, X.J., Symans, M.D., O'Rourke, M.J., Abdoun, T.H., O'Rourke, T.D., Palmer, M.C., & Stewart, H.E. (2013). Numerical modeling of buried HDPE pipelines subjected to normal faulting: A case study. *Earthquake Spectra*, 29, 609–632. doi: 10.1193/1.4000137